Supporting Information for:

Adsorption of organic compounds by biomass chars: direct role of aromatic condensation (ring cluster size) revealed by experimental and theoretical studies

Jingjing Yang[1], *Joseph J. Pignatello*[2*], *Kun Yang*[3], *Wenhao Wu*[3], *Guining Lu*[1,4], *Lijuan Zhang*[5], *Chen Yang*[1,4*], *Zhi Dang*[1,4]

Submitted to

Environmental Science & Technology

[1] School of Environment and Energy, South China University of Technology, Guangzhou 510006, China

[2] Department of Environmental Sciences, The Connecticut Agricultural Experiment Station, 123 Huntington St., New Haven, Connecticut, 06511, United States

[3] Department of Environmental Science, Zhejiang University, Hangzhou 310058, China

[4] Key Laboratory of Pollution Control and Ecosystem Restoration in Industry Clusters, Ministry of Education, Guangdong, Guangzhou 510006, China

[5] School of Chemistry and Chemical Engineering, South China University of Technology, Guangzhou 510006, China

*Corresponding author:

cyanggz@scut.edu.cn (Chen Yang); joseph.pignatello@ct.gov (Joseph J. Pignatello)

33 pages; 12 tables; 17 figures

Text S1 ***Preparation and characterization of chars***

Chars were prepared by placing a covered ceramic crucible tightly compacted to capacity with bamboo chips in a muffle furnace held at 200, 250, 300, 400, 550, or 700 ℃ for 6 h. No effort was made to control furnace headspace gas composition, so some leakage of air into the crucible during pyrolysis was likely. This is realistic since biochars and natural chars are seldom formed under strictly anoxic conditions. Chars were demineralized with 1 M HCl solution for 12 h, rinsed repeatedly with ultrapure water (Milli-Q, Millipore), and dried at 80 ℃ before storage in sealed glass containers. Experiments commenced several months after production. Elemental analysis (Table S2) was measured using a Flash EA 1112 CHN elemental analyzer (Thermo Finningan). Micropore size distribution (Fig. 1b) and specific surface area (SSA) (Table S2) were calculated by DFT and Monte Carlo Methods from the CO_2 adsorption isotherm (Autosorb IQ-MP Viton, Anton-Paar, USA) at 273 K following outgassing at 453 K. N_2 B.E.T. surface area of chars (Table S2) were calculated based N_2 isotherms at 77 K by Brunauer-Emmett-Teller (B.E.T.) theory.

Text S2 ***Sorption***

Batch adsorption experiments were conducted in 40-ml (naphthalene), 100-ml (phenanthrene), 250-ml (pyrene), or 8-ml (all other compounds) flame-sealed glass ampules. Solid-to-solution ratios were adjusted to achieve at least 20% uptake of added compound. Stock solutions of test compounds were prepared in purified water containing 0.01 M $CaCl_2$, except for PAHs, which were prepared in methanol and then diluted to different initial concentrations with 0.01 M $CaCl_2$. The volume ratio of methanol to water in the final solution was kept below 0.5% to avoid cosolvent effects. Water used in this study was purified by a Milli-Q system (18.2 MΩ•cm). To maintain the phenols in their neutral form, the pH of the mixtures was adjusted with dilute NaOH or HCl: to pH 4.0 for 2-chlorophenol, 2,4-dichlorophenol, 2-nitrophenol, 3-nitrophenol, and 4-nitrophenol; or to pH 8.0 for aniline and 4-methylphenol. For other compounds, the final solution pH was maintained at 6.5-7.5. The suspensions were placed in a rotating mixer at 150 rotations per minute for 5 days. Preliminary kinetic experiments showed 5 days was

sufficient to reach a plateau in the liquid-phase concentration (Figure S3). After the 5-day period, the solid and solution phases were separated by centrifugation (3500 revolutions per min, 20 min). Liquid-phase concentrations of PAHs were quantified using Agilent 1200 high-performance liquid chromatography with a reverse-phase C_{18} column and a fluorescence detector. Concentrations of other chemicals were determined by UV-visible spectrophotometry (Shimadzu, UV-2450, Tokyo, Japan) at their maximum absorption wavelengths listed in Table S1. The uncertainties in the measurements were below 4%. The sorbed concentration was calculated by the difference between the amount added and the amount remaining in solution.

Table S1. List and selected physicochemical properties of the test compounds (sources and purities were given previously.[3])

Compounds	MW [a]	λ_{max} [b]	pK_a [c]	$T_{melting}$ [d]	ΔH [e]	$C_W^{sat}(s)$ [f]	Sub-cooled water solubility C_W^{sat} (L) [g]
Aniline	93.13	230	4.6	-6.2	/	34160	/
2-chloroaniline	128.58	232	2.66	-1.9	/	5700	/
2-nitroaniline	138.13	223	-0.29	71.2	16110	1260	3013
3-nitroaniline	138.13	225	2.5	114	23680	900	8089
4-nitroaniline	138.13	380	1	147	21090	600	7095
Phenol	94.11	269	9.9	40.9	11290	80190	100987
2-chlorophenol	128.56	273	8.44	9.8	/	28500	/
4-chlorophenol	128.56	225	9.38	42.7	14070	26300	36149
4-methylphenol	108.13	276	10.14	35.8	11890	23000	27198
2-nitrophenol	139.11	277	7.17	44.8	17440	2100	3254
3-nitrophenol	139.11	273	8.28	96.8	19200	14000	62942
4-nitrophenol	139.11	317	7.15	113.8	18250	16000	86661
2,4-dichlorophenol	163	245	7.9	44.8	20090	4600	7619
Nitrobenzene	123.11	269	/	5.7	/	1936	/
4-nitrotoluene	137.14	284	/	51.6	16810	340	592
4-chloronitrobenzene	157.56	279	/	83.5	20780	224.8	889
1,2-dinitrobenzene	168.11	255	/	116.9	22680	133	1148
1,3-dinitrobenzene	168.11	242	/	89.7	17370	574.9	2005
1,4-dinitrobenzene	168.11	266	/	173.5	28130	69	3000
Naphthalene	128.18	Excitation:218; Emission:324	/	78.2	19120	31.7	102
Phenanthrene	178.23	Excitation:250; Emission:366	/	99.2	16470	1.29	4.85
Pyrene	202.26	Excitation:238; Emission:373	/	151.2	17110	0.135	1.05

[a] MW: molecular weight (g mol^{-1}); [b] λ_{max}: maximum absorption wavelength (nm); [c] pK_a: dissociated constant; [d] $T_{melting}$: melting points of compounds, ℃; [e] Molar enthalpy of fusion (J mol^{-1}), data from reference 14; [f] $C_W^{sat}(s)$: observed water solubility at 25 ℃ (mg L^{-1});

[g] Subcool water solubility (mg L^{-1}) for compounds in the crystalline state at 298 K was calculated by the equations:

$\Delta_{fus}G = \frac{\Delta\overline{H}_A^{fus} \cdot (T_{mp} - T)}{T_{mp}}$ and $C_w^{sat}(L) = C_w^{sat}(s) \cdot \exp(\Delta_{fus}G / RT)$ [1, 4]

Table S2. Select physical-chemical properties of chars.[a]

Char	C (%)	H (%)	O (%)	N (%)	Ash (%)	H/C	N_2 B.E.T. ($m^2\ g^{-1}$)	CO_2 specific surface area, CO_2-SSA ($m^2\ g^{-1}$)	CO_2 pore volume, $V_{micropore}$ ($cm^3\ g^{-1}$)	Total aromatic C content, F_{ar} (%)	$F_{ar,b}$ (%)	χ_b [c]	Ave number of C per ring cluster
Ba200	52.6	5.67	40.9	0.070	0.72	1.29	4.56	91.4	0.034	38.0	8.2	0.22	11
Ba250	60.6	4.46	33.0	0.421	1.49	0.883	4.82	160	0.053	56.0	16.6	0.30	15
Ba300	71.2	3.90	24.0	0.260	0.65	0.710	5.39	307	0.090	71.0	28.0	0.39	20
Ba400	72.3	2.72	21.4	0.679	2.94	0.451	7.36	402	0.112	81.6	36.3	0.45	22
Ba550	79.4	2.18	14.0	0.963	3.49	0.329	448	545	0.162	89.9	47.8	0.53	28
Ba700	87.2	1.43	7.44	0.525	3.38	0.197	511	636	0.187	85.8	59.1	0.69	63

[a]: The C, H, and N contents were measured using a Flash EA 1112 CHN elemental analyzer (Thermo Finningan). Ash contents were determined by heating the biochar at 850 ℃ for 1 h in a muffle furnace. The oxygen content was calculated by mass difference. Nitrogen B.E.T. specific surface area (Table S2) was calculated by the Brunauer-Emmett-Teller (BET) theory for N_2 adsorption isotherm at $0.05 \leq p/p_0 \leq 0.3$. The N_2 B.E.T. specific surface area is complicated by the kinetic inaccessibility of some of the pores at 77 K[5 6].

Table S3. Dubinin-Ashtahkov model parameters for select test compounds on chars [a]

Compounds	Char	$\log Q^0$ (Q^0, mg g^{-1})	E_{DA} (kJ mol^{-1})	b	r^2	N
Aniline	Ba200	2.445±0.151	7.04±1.46	0.76±0.11	0.998	15
	Ba250	2.518±0.045	11.4±0.59	0.87±0.06	0.999	15
	Ba300	2.480±0.032	14.7±0.53	0.87±0.04	0.999	15
	Ba400	2.173±0.016	19.0±0.45	1.37±0.09	0.993	21
	Ba550	2.204±0.010	24.7±0.75	1.44±0.08	0.990	23
	Ba700	2.218±0.003	31.6±0.25	1.98±0.04	0.998	28
Phenol	Ba200	2.593±0.030	6.66±0.24	0.97±0.03	0.998	24
	Ba250	2.612±0.017	9.50±0.20	0.97±0.02	0.999	24
	Ba300	2.561±0.011	13.7±0.17	1.04±0.02	0.999	24
	Ba400	2.220±0.015	17.9±0.23	1.75±0.10	0.990	24
	Ba550	2.201±0.007	26.8±0.20	1.79±0.06	0.996	24
	Ba700	2.262±0.083	33.3±0.26	2.26±0.08	0.995	21
4-nitrophenol	Ba200	2.994±0.043	8.27±0.33	1.07±0.03	0.999	24
	Ba250	2.954±0.030	11.2±0.36	1.01±0.03	0.999	24
	Ba300	2.648±0.024	18.2±0.42	1.19±0.03	0.999	24
	Ba400	2.344±0.015	25.0±0.25	1.71±0.06	0.998	24
	Ba550	2.343±0.005	38.1±0.16	1.68±0.03	0.999	24
	Ba700	2.249±0.079	51.4±1.20	2.11±0.08	0.995	26
Nitrobenzene	Ba200	1.928±0.014	6.44±0.10	0.92±0.02	1.000	23
	Ba250	2.262±0.013	8.90±0.11	0.92±0.02	1.000	24
	Ba300	2.454±0.026	12.9±0.32	0.90±0.05	0.998	20
	Ba400	2.208±0.012	17.2±0.19	1.29±0.05	0.998	22
	Ba550	2.302±0.010	28.0±0.75	1.33±0.07	0.992	24
	Ba700[a]	2.266±0.003	34.4±0.44	2.24±0.06	0.995	19
Naphthalene	Ba200	2.072±0.218	5.27±1.20	0.91±0.12	0.995	20
	Ba250	1.642±0.072	10.6±0.73	1.17±0.10	0.993	22
	Ba300	1.431±0.036	14.2±0.29	1.96±0.14	0.994	18
	Ba400	1.575±0.037	16.8±0.46	1.45±0.11	0.992	21
	Ba550	2.040±0.015	27.1±0.35	1.65±0.09	0.993	19
	Ba700	2.079±0.010	32.0±0.19	3.23±0.12	0.994	21

[a] Estimated parameter values and their standard errors were determined by commercial software (Origin 8.0) using nonlinear regression

Table S4. Results of linear regressions between E_{DA} and fraction of bridgehead carbon: $\boldsymbol{E_{DA}} = m_{DA}\boldsymbol{\chi_b} + const_{DA}$

Compounds	m_{DA}	$const_{DA}$	r^2
aniline	55.6 ± 5.51	-6.14 ± 2.90	0.97
2-chloroaniline	63.1 ± 11.7	-8.83 ± 6.17	0.9
2-nitroaniline	50.8 ± 8.81	-2.13 ± 4.64	0.91
3-nitroaniline	51.3 ± 12.2	1.87 ± 6.41	0.85
4-nitroaniline	66.6 ± 10.0	-5.37 ± 7.27	0.94
phenol	66.3 ± 10.5	-11.2 ± 5.53	0.93
2-chlorophenol	88.4 ± 10.1	-19.8 ± 5.3	0.96
4-chlorophenol	88.0 ± 17.4	-19.6 ± 9.17	0.89
4-methylphenol	80.7 ± 20.4	-17.2 ± 10.8	0.83
2,4-dichlorophenol	89.0 ± 14.9	-21.6 ± 7.86	0.92
2-nitrophenol	69.2 ± 13.6	-11.7 ± 7.17	0.89
3-nitrophenol	108 ± 11.1	-25.5 ± 5.86	0.97
4-nitrophenol	112 ± 11.8	-24.4 ± 6.24	0.97
nitrobenzene	73.3 ± 13.8	-14.6 ± 7.28	0.9
4-nitrotoluene	69.6 ± 3.27	-12.1 ± 1.72	0.99
4-chloronitrobenzne	63.7 ± 13.6	-8.25 ± 7.15	0.77
1,2-dinitrobenzene	55.7 ± 9.66	-5.99 ± 5.09	0.91
1,3-dinitrobenzene	81.7 ± 5.98	-15.9 ± 3.15	0.98
1,4-dinitrobenzene	65.1 ± 13.4	-6.30 ± 7.07	0.88
naphthalene	62.0 ± 13.4	-9.39 ± 7.09	0.87
phenanthrene	59.7 ± 6.25	-8.01 ± 3.30	0.97
pyrene	53.5 ± 13.2	-5.95 ± 6.96	0.84

Table S5. The average site energy $E_{DA,mean}$ (kJ mol^{-1}) of chars for 22 organic compounds.

Compounds	Ba200	Ba250	Ba300	Ba400	Ba550	Ba700
Phenol	4.84	6.14	7.34	7.77	9.98	33.4
2-chlorophenol	10.5	5.74	7.63	8.59	9.77	13.3
4-chlorophenol	13.4	6.66	7.64	8.42	9.02	13.5
4-methylphenol	4.5	6.63	8.27	8.46	10.6	13.4
2,4-dichlorophenol	6.00	7.78	8.37	8.73	11.4	11.5
2-nitrophenol	5.32	6.66	8.27	8.33	11.2	12.4
3-nitrophenol	8.23	9.24	11.6	11.9	14.1	16.0
4-nitrophenol	9.32	10.2	14.2	13.6	15.6	16.7
Aniline	5.76	6.80	9.12	7.59	8.98	12.4
2-chloroaniline	4.83	6.12	9.04	6.73	8.07	10.7
2-nitroaniline	6.64	8.42	9.68	10.2	10.5	13.8
3-nitroaniline	10.7	12.3	14.6	12.3	12.6	15.9
4-nitroaniline	10.4	12.0	13.3	14.1	16.4	19.5
Nitrobenzene	4.26	5.74	6.85	7.96	10.3	13
4-nitrotoluene	5.92	6.56	8.68	9.64	10.3	12.0
4-chloronitrobenzene	8.96	9.41	10.3	12.4	13.9	14.9
1,2-dinitrobenzene	10.2	10.8	12.8	11.6	12.7	15.3
1,3-dinitrobenzene	7.30	8.58	9.74	10.6	11.6	13.6
1,4-dinitrobenzene	13.9	14.9	16.7	16.3	18.1	19.0
Naphthalene	8.49	7.74	8.58	9.29	11.2	13.7
Phenanthrene	6.23	6.69	7.61	8.14	9.86	12.4
Pyrene	9.76	10.7	10.1	9.86	11.0	11.6

$E_{DA,mean}$ were calculated from equations those are cited from ref [7]:

$$E_{DA,mean} = \frac{\int_{\varepsilon_h}^{\varepsilon_l} \frac{(\varepsilon / E_{DA})^b}{10^{[(\varepsilon/E_{DA})^b]}} d_\varepsilon}{\int_{\varepsilon h}^{\varepsilon_l} \frac{\varepsilon^{b-1}}{E_{DA}^b \ln 10^{[(\varepsilon/E_{DA})^b]}} d_\varepsilon}$$

$$\varepsilon = -RT \ln \frac{C_e}{C_W^{sat}(L)}$$

where C_e (mg/L) is the equilibrium aqueous concentration; $C_W^{sat}(L)$ (mg L^{-1}) is the liquid or sub-cooled liquid water solubility at 298 K, R=8.314×10^{-3} kJ/(mol K); T=298 K. ε_l and ε_h are ε values at the lowest concentration and the highest concentration in the experimental concentration range, respectively.

Table S6. Resutls of linear regression between sorption capacity (Q^0) and χ_b

Compounds	r^2	p value	Compounds	r^2	p value
Aniline	0.57	0.08	4-nitrophenol	0.78	0.02
2-chloroaniline	0.41	0.17	2,4-dichlorophenol	0.674	0.05
2-nitroaniline	0.04	0.17	Nitrobenzene	0.12	0.51
3-nitroaniline	0.08	0.58	4-nitrotoluene	0.55	0.09
4-nitroaniline	0.14	0.47	4-chloronitrobenzene	0.88	<0.01
Phenol	0.67	0.05	1,2-dinitrobenzene	0.12	0.50
2-chlorophenol	0.73	0.03	1,3-dinitrobenzene	0.54	0.10
4-chlorophenol	0.71	0.04	1,4-dinitrobenzene	0.76	0.02
4-methylphenol	0.11	0.53	Naphthalene	0.09	0.56
2-nitrophenol	0.11	0.52	Phenanthrene	0.16	0.43
3-nitrophenol	0.35	0.22	Pyrene	0.22	0.34

All linear regression and significance test were obtained by a commercial software program (SPSS 19.0).

Table S7. Computational binding energies (E_{bd}) and minimum distances for the sheet-compound configurations shown in Fig. S13

	Sheet (Ha)	Compound (Ha)	Sheet-Compound (Ha)	E_{bd} (kJ mol^{-1})	Distance [b] (Å)
			Phenol		
Ba200[a]	-385.5381	-307.2240	-692.7678	-14.7	3.380
Ba250	-539.0425	-307.2240	-846.2741	-19.7	3.400
Ba300	-615.2223	-307.2240	-922.4561	-25.2	3.262
Ba400	-844.9077	-307.2240	-1152.1438	-31.2	3.242
Ba550	-1150.7556	-307.2240	-1457.9940	-37.9	3.174
Ba700	-2067.1767	-307.2240	-2374.4182	-46.0	3.148
$C_{66}H_{20}$	-2525.3754	-307.2240	-2832.6170	-46.1	3.093
$C_{90}H_{24}$	-3441.7623	-307.2240	-3749.0042	-46.9	3.033
			Aniline		
Ba200	-385.5381	-287.3591	-672.9046	-19.5	3.311
Ba250	-539.0425	-287.3591	-826.4123	-28.0	3.236
Ba300	-615.2223	-287.3591	-902.5936	-29.8	3.210
Ba400	-844.9077	-287.3591	-1132.2814	-38.5	3.209
Ba550	-1150.7556	-287.3591	-1438.1312	-43.2	3.142
Ba700	-2067.1767	-287.3591	-2354.5553	-51.2	3.100
$C_{66}H_{20}$	-2525.3754	-287.3591	-2812.7527	-47.7	3.128
$C_{90}H_{24}$	-3441.7623	-287.3591	-3729.1410	-51.3	3.109
			Nitrobenzene		
Ba200	-385.5381	-436.4499	-821.9991	-29.3	3.310

Ba250	-539.0425	-436.4499	-975.5041	-30.8	3.267
Ba300	-615.2223	-436.4499	-1051.6867	-38.4	3.218
Ba400	-844.9077	-436.4499	-1281.3731	-40.9	3.255
Ba550	-1150.7556	-436.4499	-1587.2232	-46.6	3.239
Ba700	-2067.1767	-436.4499	-2503.6469	-53.5	3.154
$C_{66}H_{20}$	-2525.3754	-436.4499	-2961.8456	-53.3	3.103
$C_{90}H_{24}$	-3441.7623	-436.4499	-3878.2323	-52.8	3.081
			Naphthalene		
Ba200	-385.5381	-385.5379	-771.0834	-19.2	3.377
Ba250	-539.0425	-385.5379	-924.5910	-27.7	3.335
Ba300	-615.2223	-385.5379	-1000.7734	-35.7	3.266
Ba400	-844.9077	-385.5379	-1230.4629	-45.6	3.230
Ba550	-1150.7556	-385.5379	-1536.3134	-52.2	3.228
Ba700	-2067.1767	-385.5379	-2452.7403	-67.5	3.143
$C_{66}H_{20}$	-2525.3754	-385.5379	-2910.9401	-70.3	3.092
$C_{90}H_{24}$	-3441.7623	-385.5379	-3827.3281	-73.0	3.098
			4-Nitrophenol		
Ba200	-385.5381	-511.6499	-897.2000	-31.3	3.249
Ba250	-539.0425	-511.6499	-1050.7052	-33.4	3.406
Ba300	-615.2223	-511.6499	-1126.8858	-37.4	3.226
Ba400	-844.9077	-511.6499	-1356.5742	-43.6	3.190
Ba550	-1150.7556	-511.6499	-1662.4216	-42.3	3.237
Ba700	-2067.1767	-511.6499	-2578.8487	-57.9	3.050
$C_{66}H_{20}$	-2525.3754	-511.6499	-3037.0465	-55.6	3.114
$C_{90}H_{24}$	-3441.7623	-511.6499	-3953.4331	-54.7	3.124

[a] Ba200-Ba700 and $C_{66}H_{20}$ and $C_{90}H_{24}$ correspond, respectively, to structures **A-H** in Fig.4a of main paper.

[b]Distance from the center of the benzene ring of the compounds to the plane of the aromatic sheet.

Table S8. Results of linear regression between E_{bd} and mole fraction of bridgehead aromatic carbon: $\boldsymbol{E_{bd}} = m_{bd}\boldsymbol{\chi_b} + const_{bd}$

Compounds	m_{bd}	$const_{bd}$	r^2
Phenol	69.3 ± 2.88	0.32 ± 1.28	0.99
4-nitrophenol	55.0 ± 8.02	18.0 ± 3.56	0.90
Nitrobenzene	54.9 ± 3.89	17.0 ± 1.73	0.98
Aniline	68.0 ± 4.83	6.70± 2.14	0.98
Naphthalene	104 ± 1.90	-2.21 ± 0.84	1.00

Table S9. Static polarizability components and polarizability of polybenzeneoid hydrocarbons

Char	α_{xx} (au)	α_{yy} (au)	α_{zz} (au)	α_{PBH} (Å^3)
Ba200	176.94	128.35	66.60	18.37
Ba250	307.07	173.14	87.62	28.05
Ba300	388.77	273.29	108.54	38.06
Ba400	499.64	448.10	139.66	53.71
Ba550	591.67	542.60	155.54	63.71
Ba700	1149.09	1148.42	249.59	125.81
$C_{66}H_{20}$	1634.15	1400.71	295.92	164.52
$C_{90}H_{24}$	2798.80	2031.57	388.43	257.78

Ba200-Ba700 correspond, respectively, to structures **A-H** in Fig.4a of main paper. $\alpha_{PBH} = (\alpha_{xx} + \alpha_{yy} + \alpha_{zz})/3$. au, atomic units.

Table S10. Computational binding energies ($\boldsymbol{E_{bd}}$) of phenol adsorption between dual parallel PBH sheets (Ba400, **D**) at different intersheet distances (Ba400, **D**)

Distance (nm)	Sheet (Ha)	Phenol (Ha)	Sheet-Phenol (Ha)	$\boldsymbol{E_{bd}}$ (kJ mol^{-1})
0.45	-1689.8218	-307.2240	-1996.7854	683
0.50	-1689.8181	-307.2240	-1996.9432	260
0.55	-1689.8210	-307.2240	-1997.0279	45.0
0.58	-1689.8197	-307.2240	-1997.0500	-18.7
0.60	-1689.8185	-307.2240	-1997.0581	-40.9
0.62	-1689.8179	-307.2240	-1997.0613	-50.9
0.64	-1689.8176	-307.2240	-1997.0629	-55.7
0.66	-1689.8173	-307.2240	-1997.0630	-56.8
0.68	-1689.8171	-307.2240	-1997.0616	-53.6
0.70	-1689.8169	-307.2240	-1997.0599	-49.7
0.75	-1689.8165	-307.2240	-1997.0545	-36.4
0.80	-1689.8163	-307.2240	-1997.0535	-34.5
1.0	-1689.8159	-307.2240	-1997.0524	-32.7
2.0	-1689.8157	-307.2240	-1997.0517	-31.3
single sheet	-844.9078	-307.2240	-1152.1438	-31.2

Table S11. Binding energies (E_{bd}) of phenol adsorption between dual parallel PBH sheets (Ba400, **D**) at an inter-sheet distance of 0.68 nm

	Sheet (Ha)	Phenol (Ha)	Sheet-Phenol (Ha)	E_{bd} (kJ mol^{-1})
Ba200	-771.0762	-307.2240	-1078.3109	-28.0
Ba250	-1078.0855	-307.2240	-1385.3230	-35.4
Ba300	-1385.1228	-307.2240	-1692.3634	-43.6
Ba400	-1689.8171	-307.2240	-1997.0616	-53.6
Ba550	-2301.5132	-307.2240	-2608.7632	-68.4
Ba700	-4134.3576	-307.2240	-4441.6117	-78.9

Table S12. Binding energies (E_{bd}) of two parallel-planar molecules adsorbed in a bilayer between parallel PBH sheets placed 1 nm apart.

	Sheet (Ha)	Compound (Ha)	Sheet-Compound (Ha)	E_{bd} (kJ mol^{-1}) per each phenol
			Phenol	
Ba400	-1689.8155	-614.4480	-2304.2903	-35.2
Ba700	-4134.3532	-614.4480	-4748.8386	-49.1
			Naphthalene	
Ba400	-1689.8171	-771.0758	-2460.9314	-50.5[a]

[a]The corresponding value for a single naphthalene molecule is -45.6 kJ mol^{-1}.

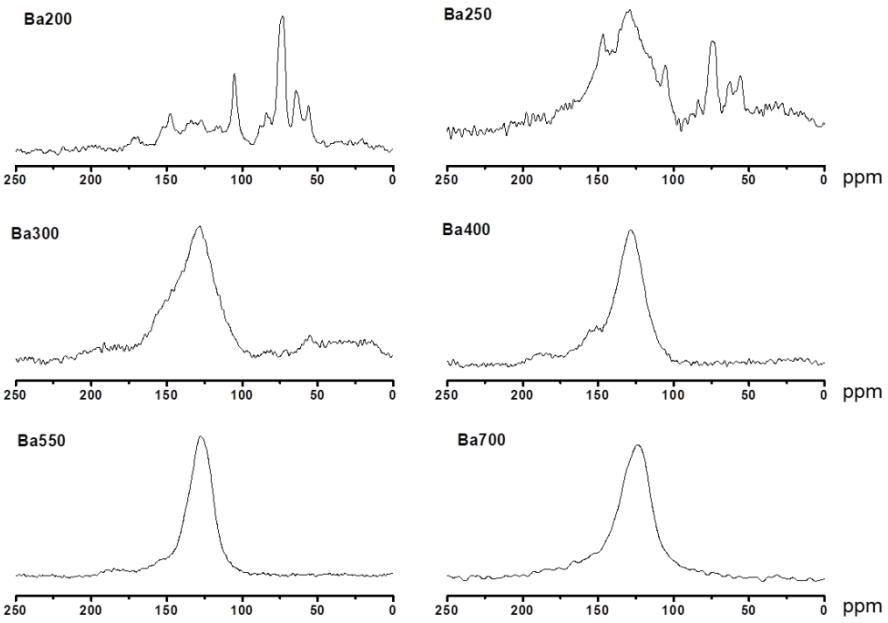

Figure S1. Solid state ^{13}C DP/MAS NMR spectra of chars

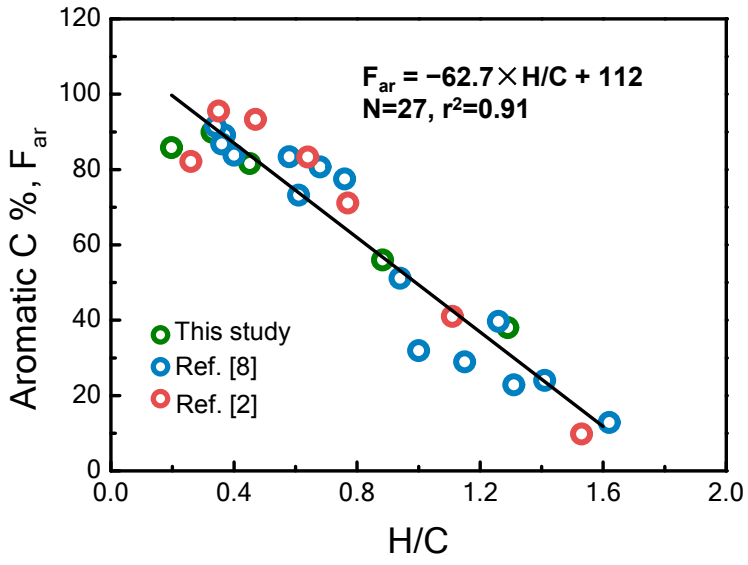

Figure S2. Correlation between the total aromatic carbon content ($\boldsymbol{F_{ar}}$) and atomic ratio of H/C for chars. Blue[8] and red points[2] are data from literatures. Black line is the linear fitting line.

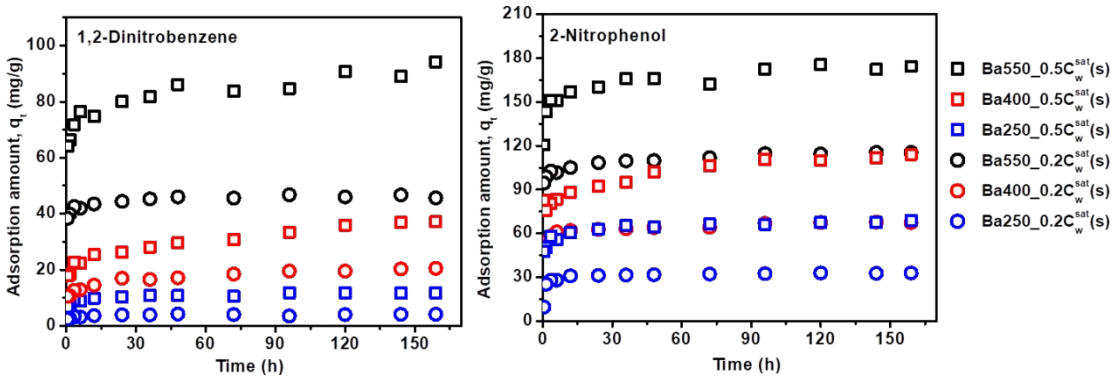

Figure S3. Preliminary kinetic experiments for two compounds with different solubilities at two initial concentrations on Ba550, Ba400 and Ba250 which represents chars produced at high HTT, medium HTT and low HTT, respectively.

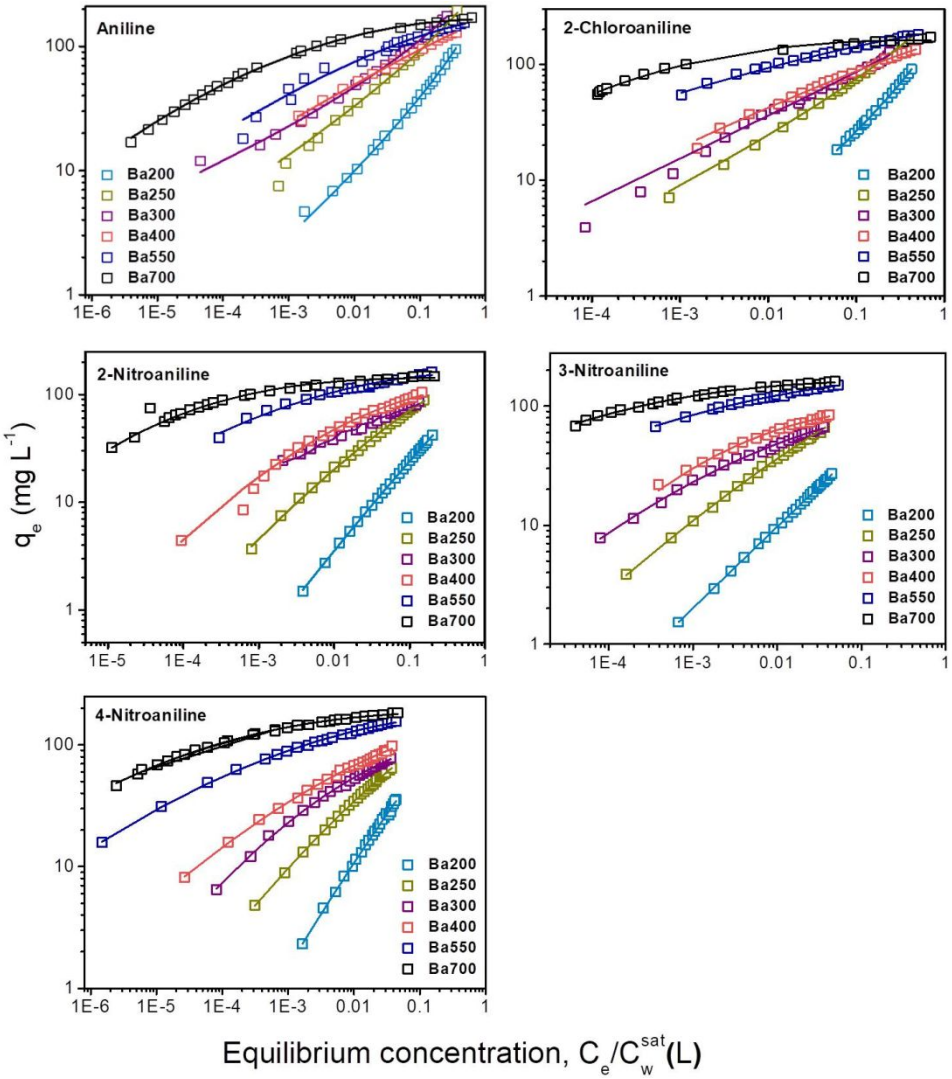

Figure S4. Adsorption isotherms of anilines on chars fit to the Dubinin-Ashtakhov model.

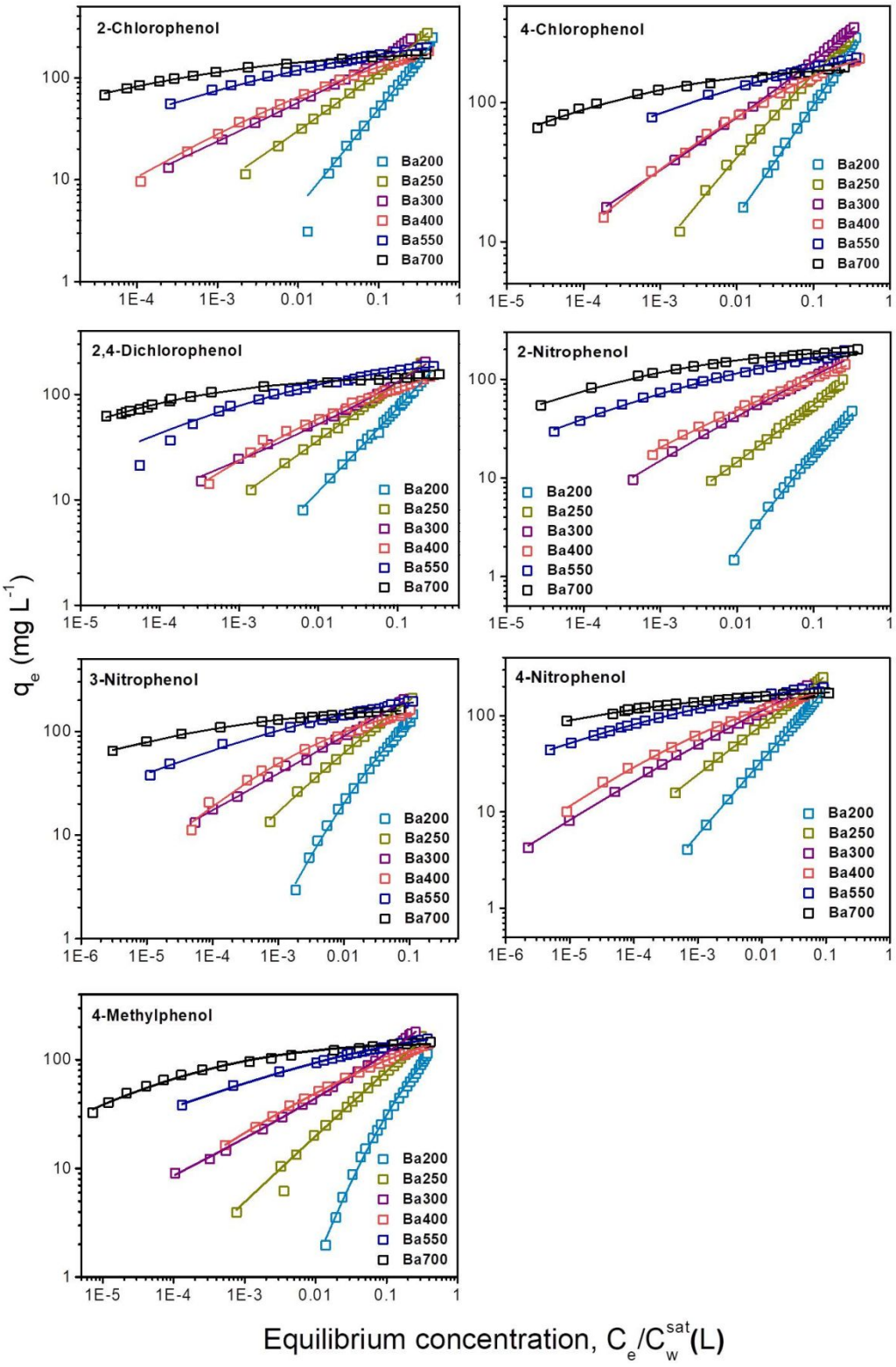

Figure S5. Adsorption isotherms of phenols on chars fit to the Dubinin-Ashtakhov model.

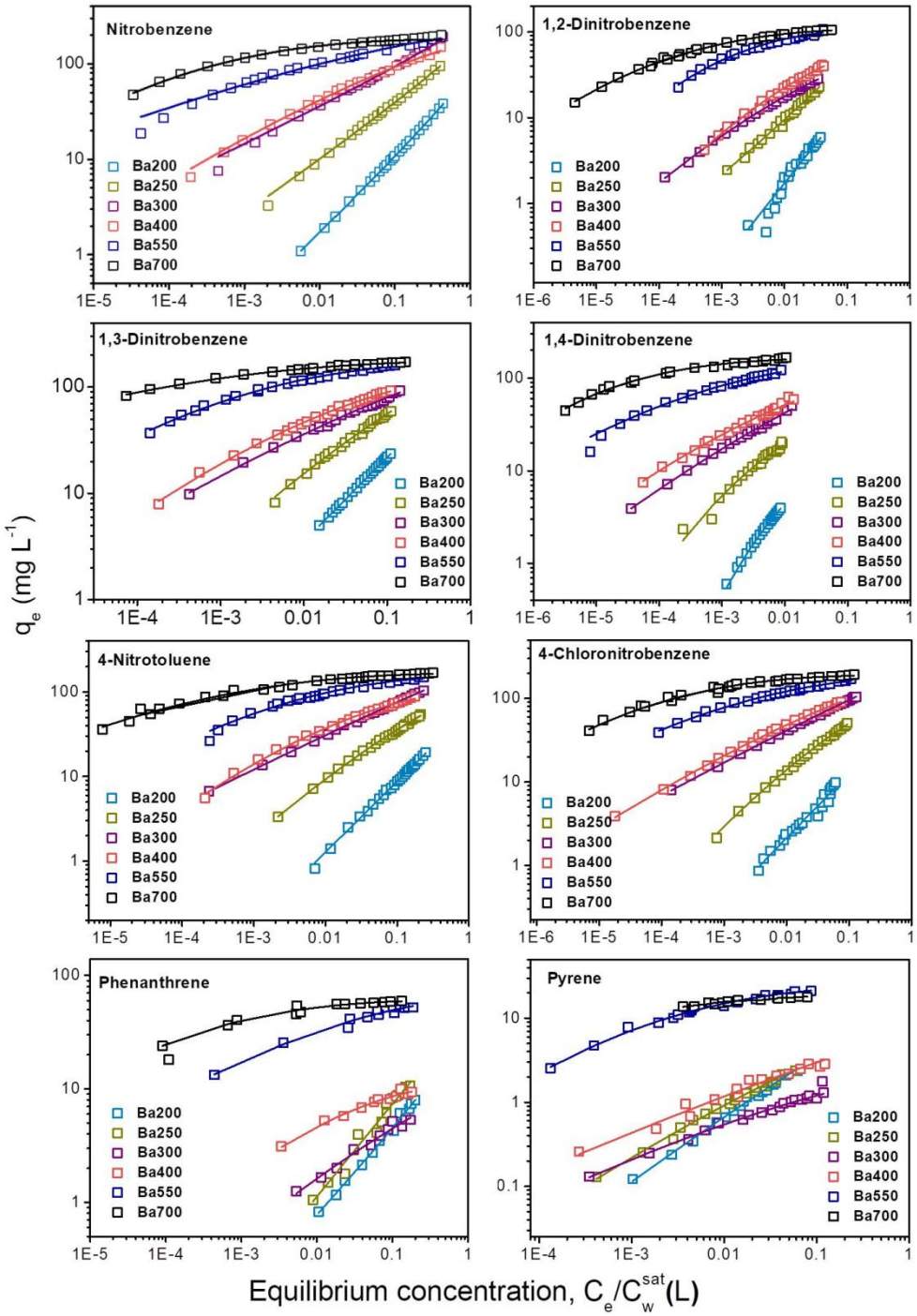

Figure S6. Adsorption isotherms of nitrobenzenes and PAHs on chars fit to the Dubinin-Ashtakhov model.

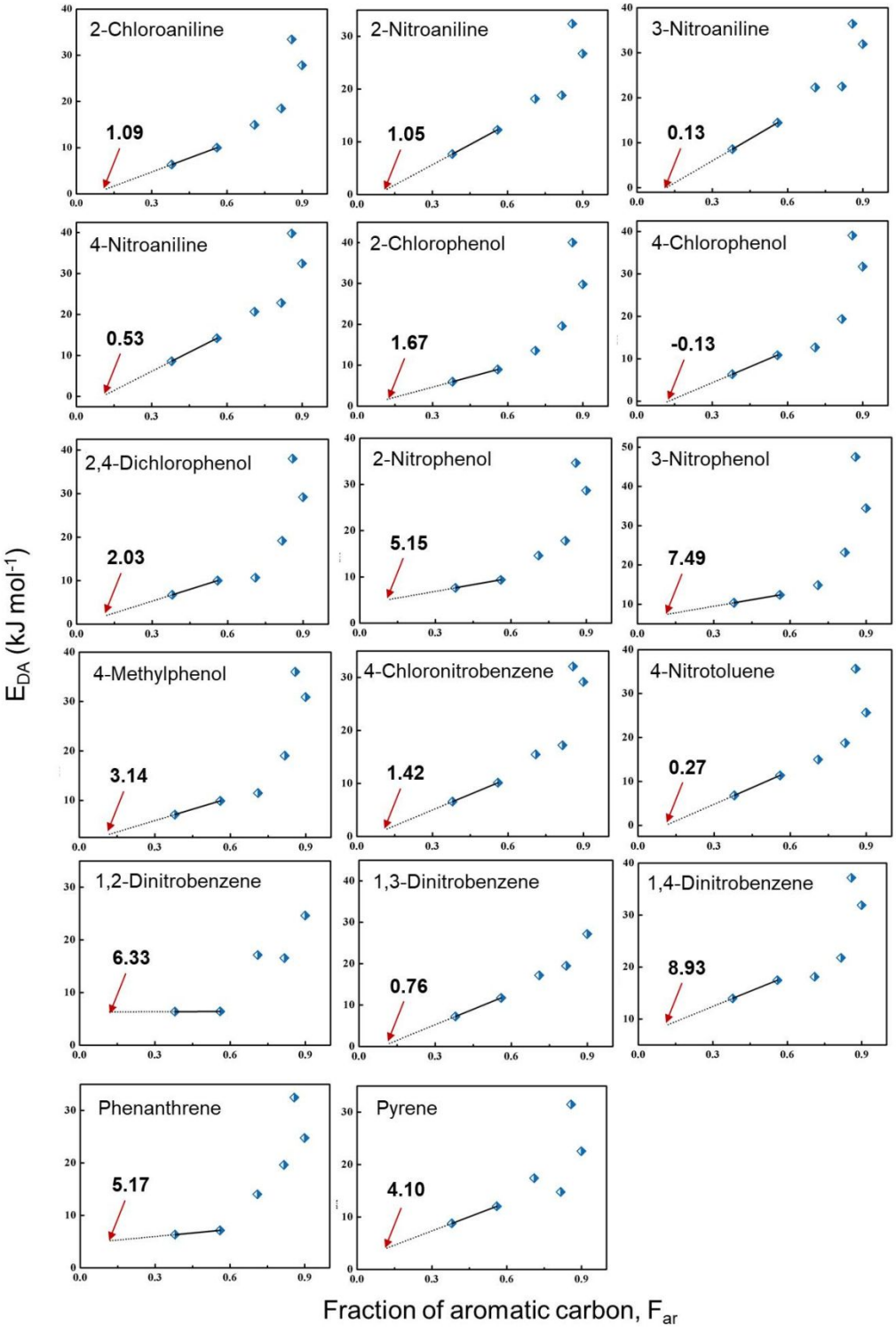

Figure S7. Correlations between the fraction of aromatic carbon (F_{ar}) and E_{DA} values. Solid lines connect Ba200 and Ba250 and dotted lines are the extraploted line to the F_{ar} corresponding to fresh bamboo (0.12, red arrows).

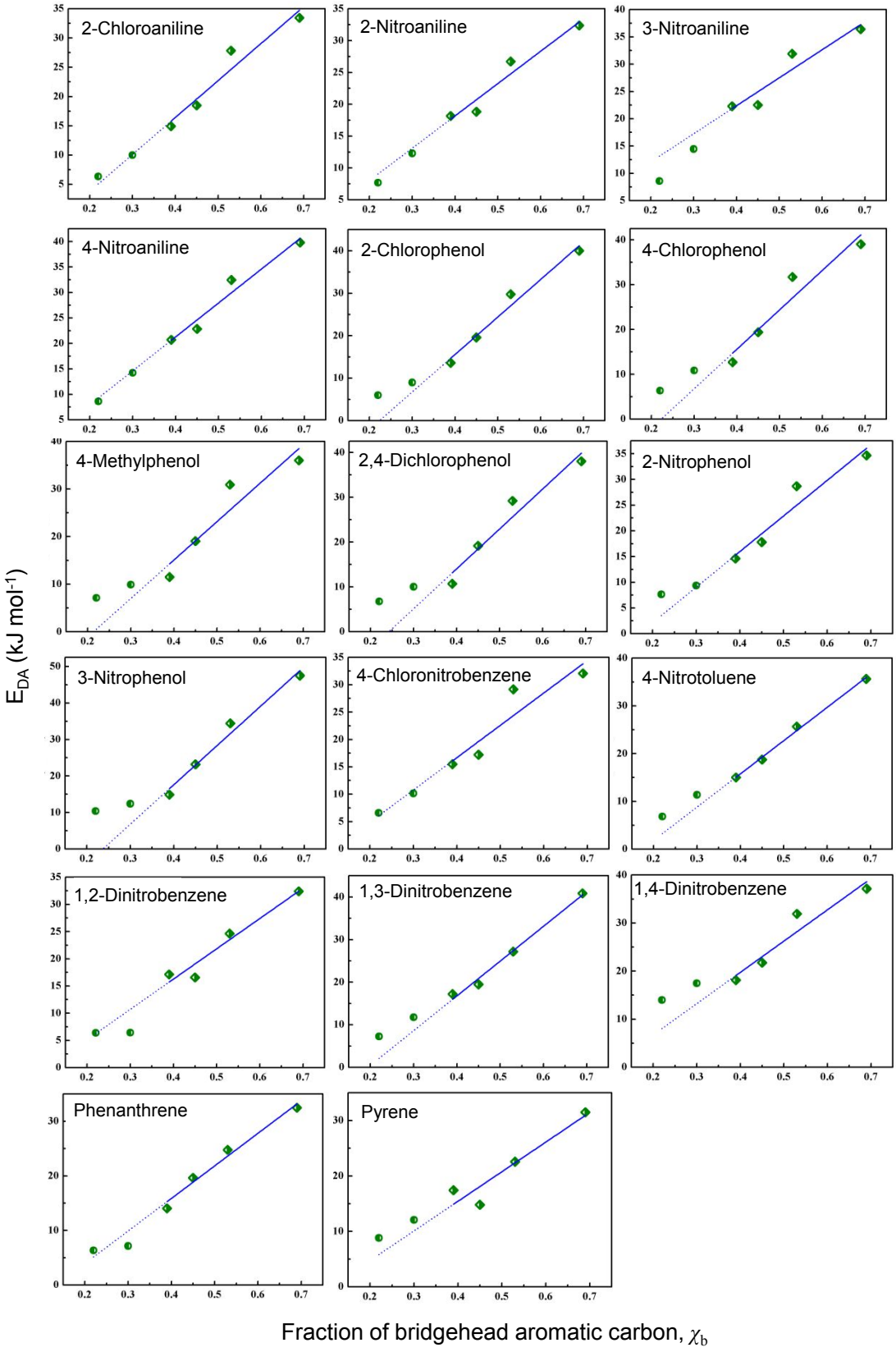

Figure S8. Correlations between fraction of bridgehead aromatic carbon and $\boldsymbol{E_{DA}}$ values. Solid lines are linear regression fits of Ba300, Ba400, Ba550 and Ba700. Dash lines are extrapolated lines from the solid lines.

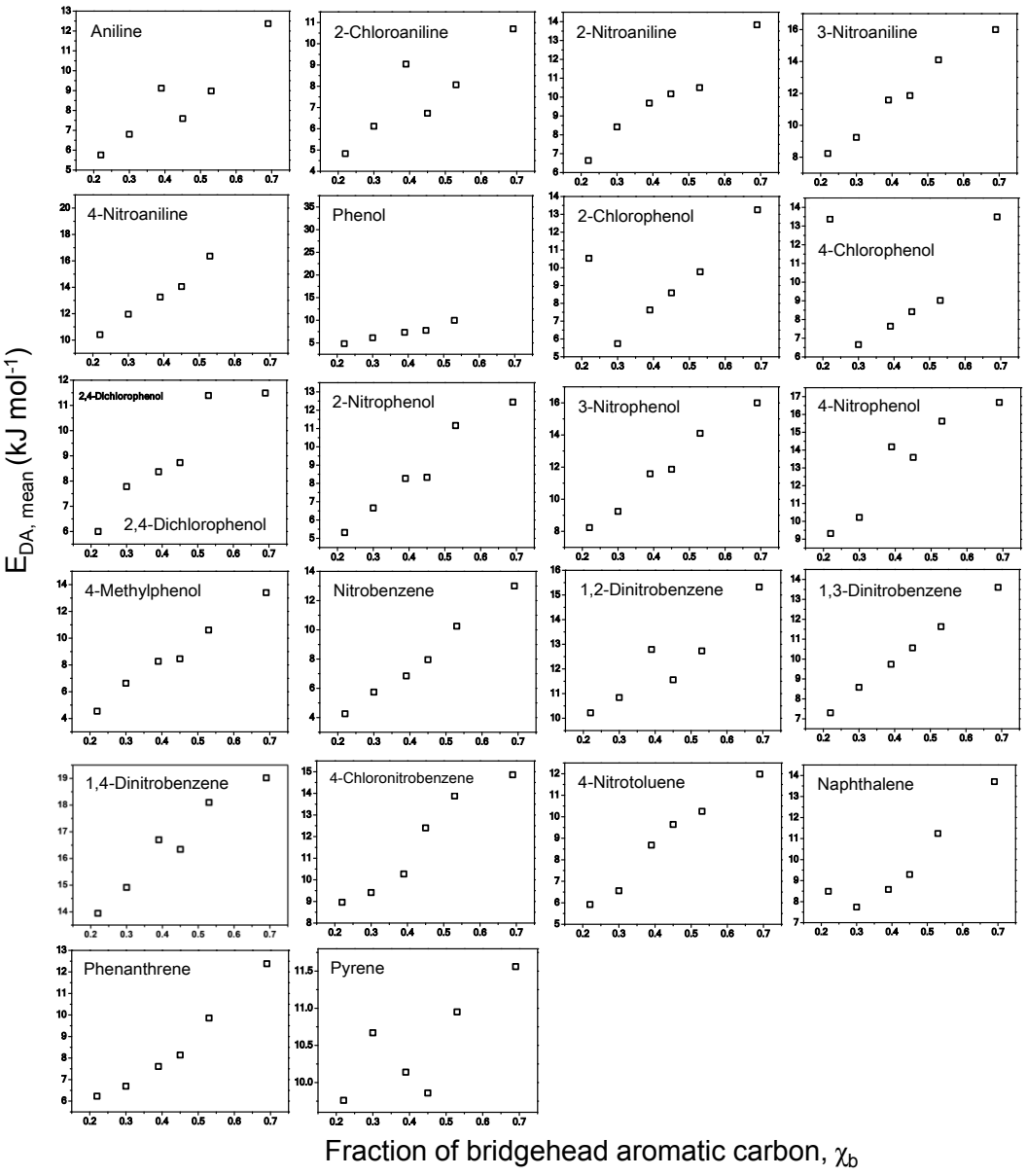

Figure S9. Correlations between fraction of bridgehead aromatic carbon (χ_b) and $E_{DA,mean}$ values listed in Table S5.

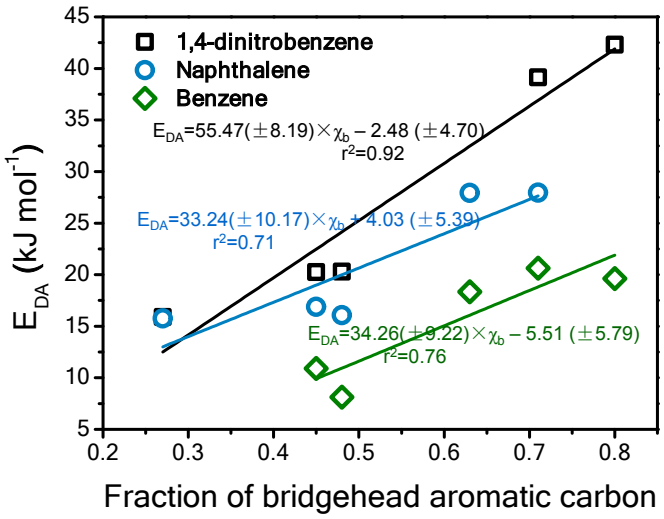

Figure S10. Correlations between sorption E_{DA} values and fraction of bridgehead aromatic carbon (χ_b) on wood chars. Data is obtained from the literature [1, 2].

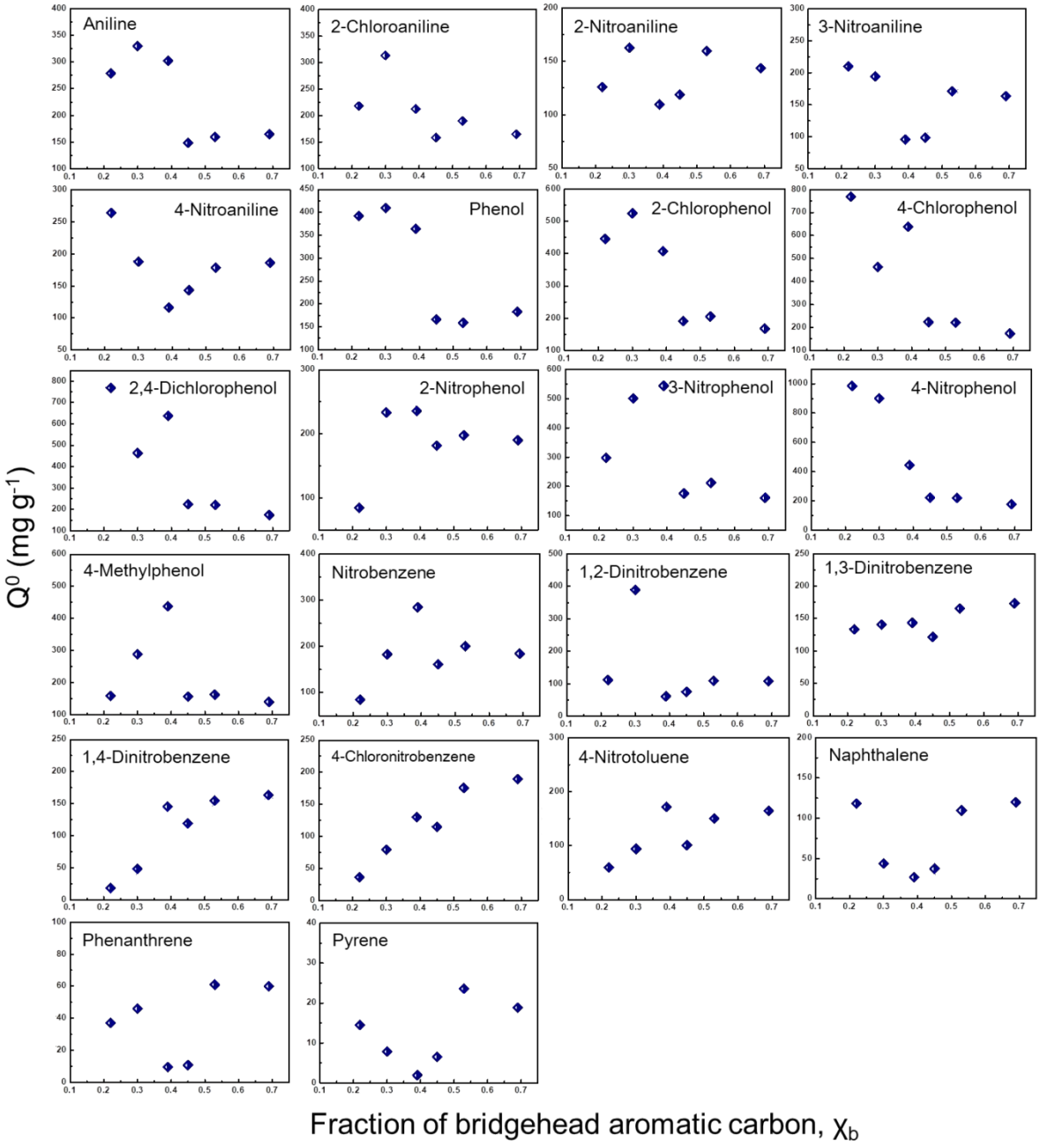

Figure S11. Correlations between sorption capacity ($\boldsymbol{Q^0}$, mg g^{-1}) and fraction of bridgehead aromatic carbon ($\boldsymbol{\chi_b}$).

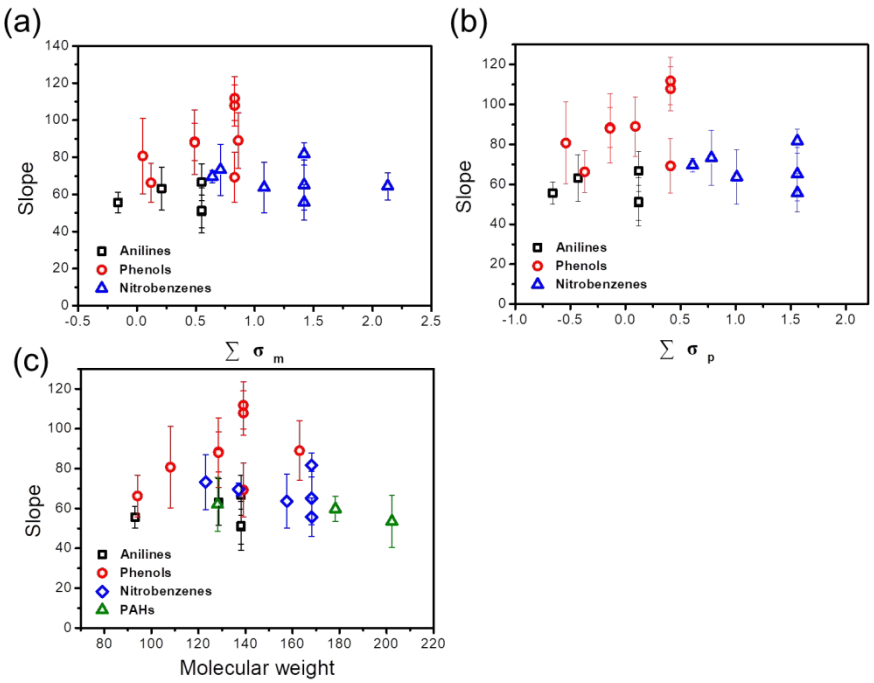

Figure S12. Correlations between the slope m_{DA} of the relationship $\boldsymbol{E_{DA}} = m_{DA}\,\boldsymbol{\chi_b} + const_{DA}$ (from Table S4) and, (a) the sum of Hammett σ_{meta}, (b) the sum of Hammett σ_{para}, or (c) the molecular weight, for 22 compounds.

(a) Phenol

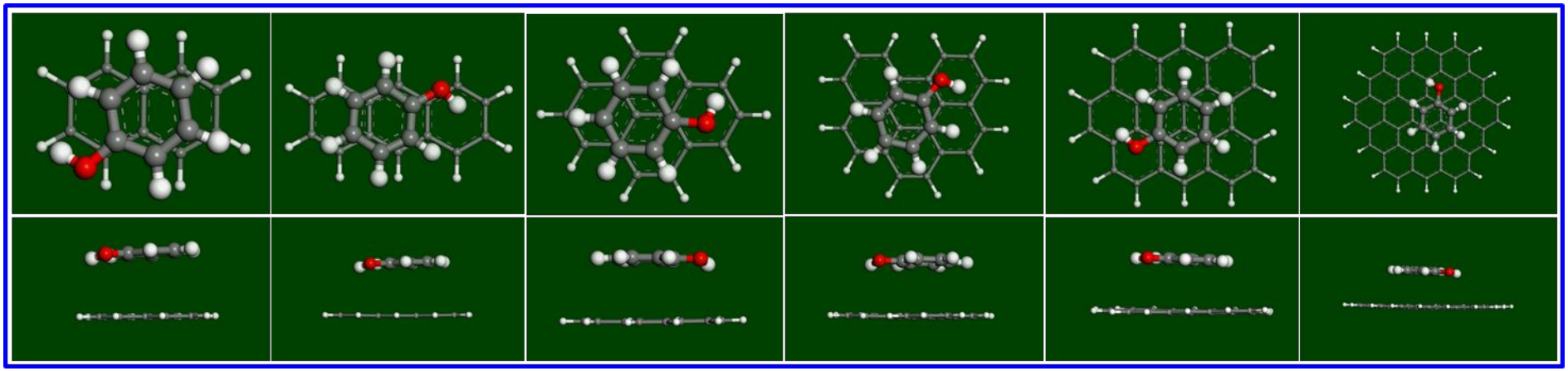

(b) Aniline

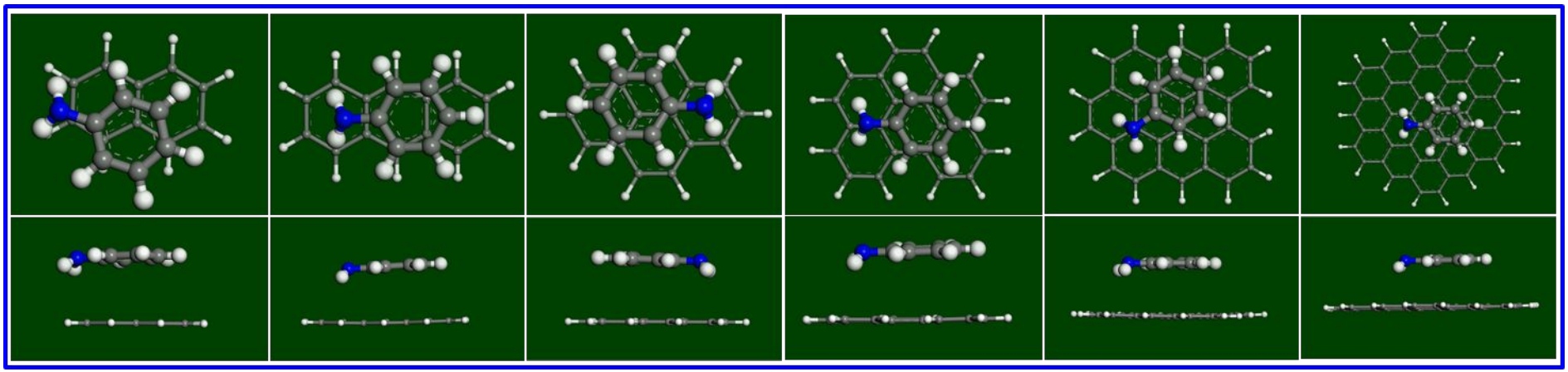

(c) Nitrobenzene

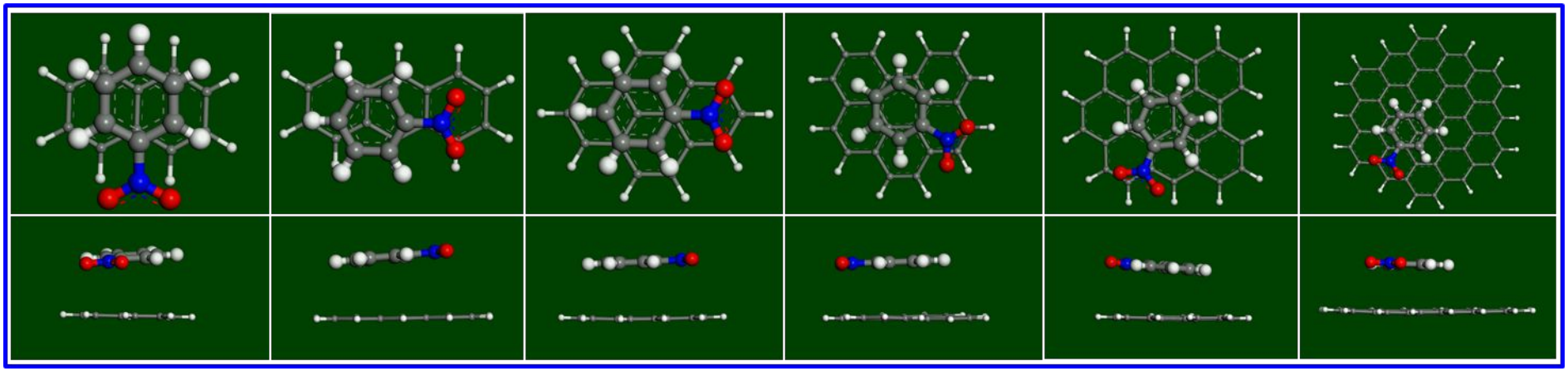

(d) Naphthalene

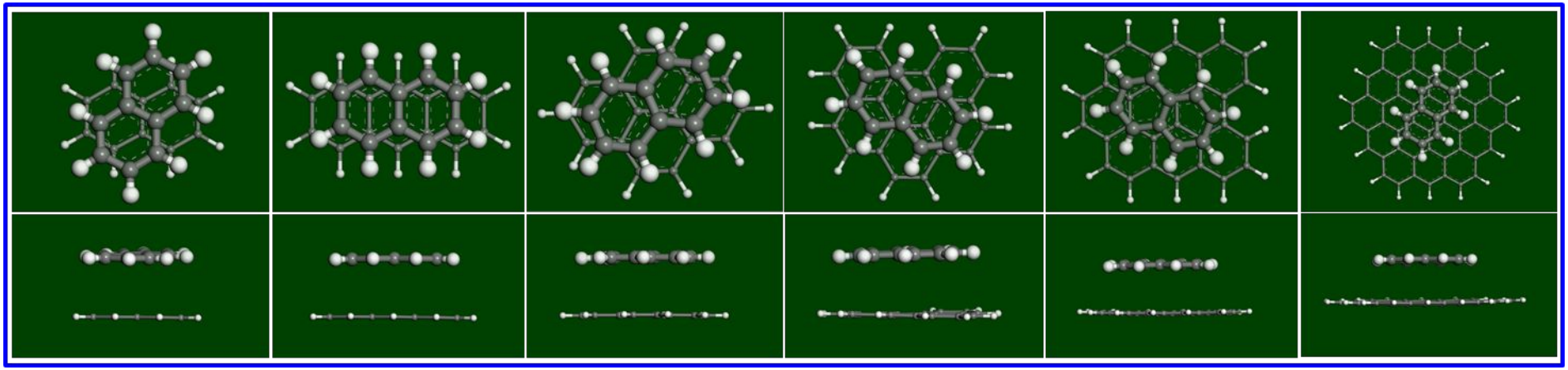

(e) 4-Nitrophenol

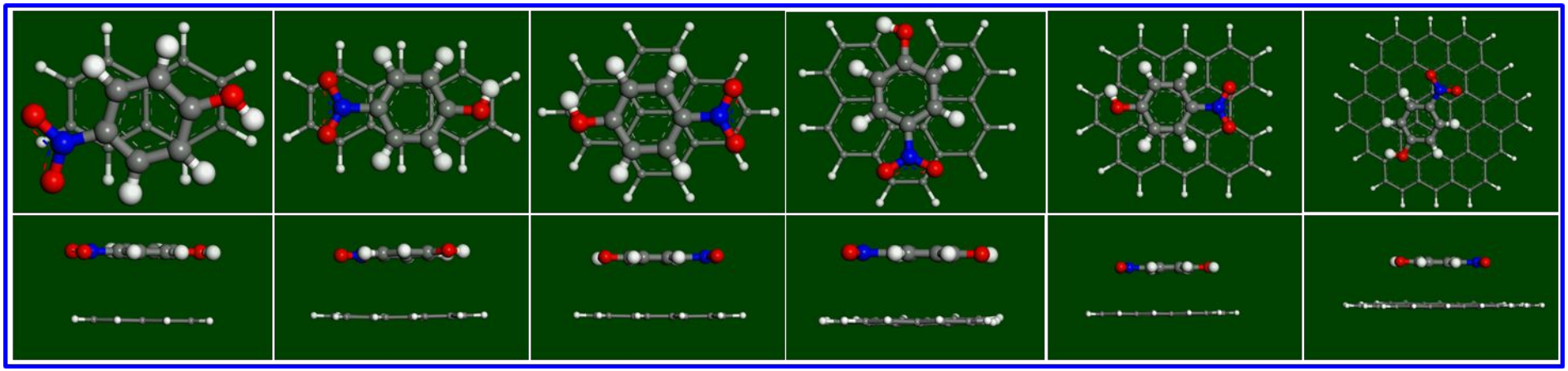

Figure S13. Simulation results for the optimized complexes. (dark gray: C; white: H; blue: N; red: O). The PBH sheets correspond, left to right, to the chars: B200, Ba250, Ba300, Ba400, Ba550, and Ba700 (structures **A-F**, Fig. 4a).

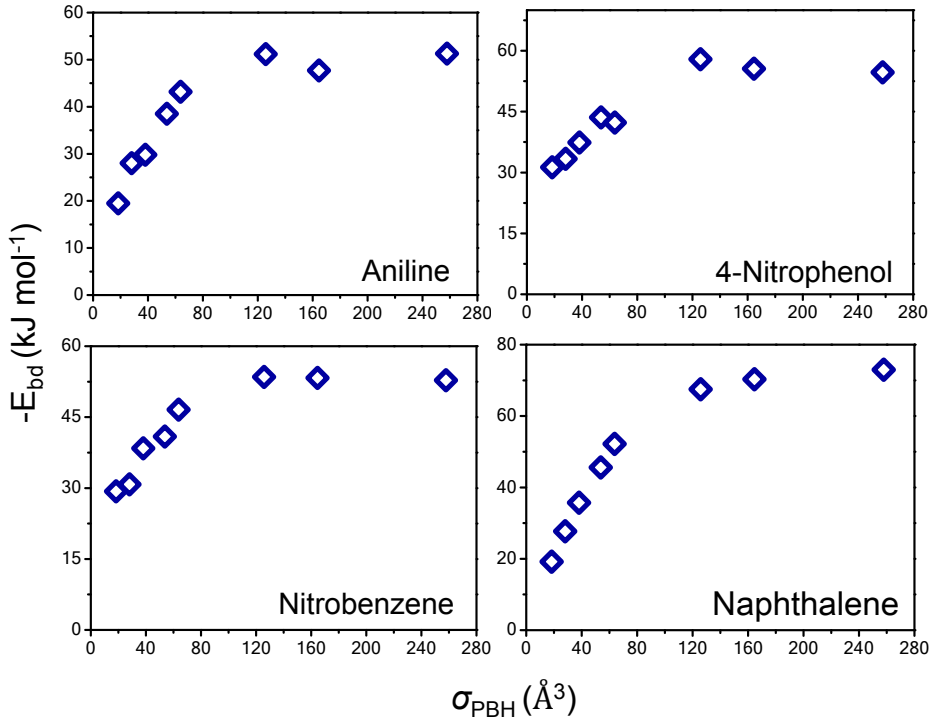

Figure S14. Correlations between static polarizability of PBH **A** – **H** (Fig. 4a) and $\boldsymbol{E_{bd}}$ for adsorption of four compounds on the single-sheet PBH.

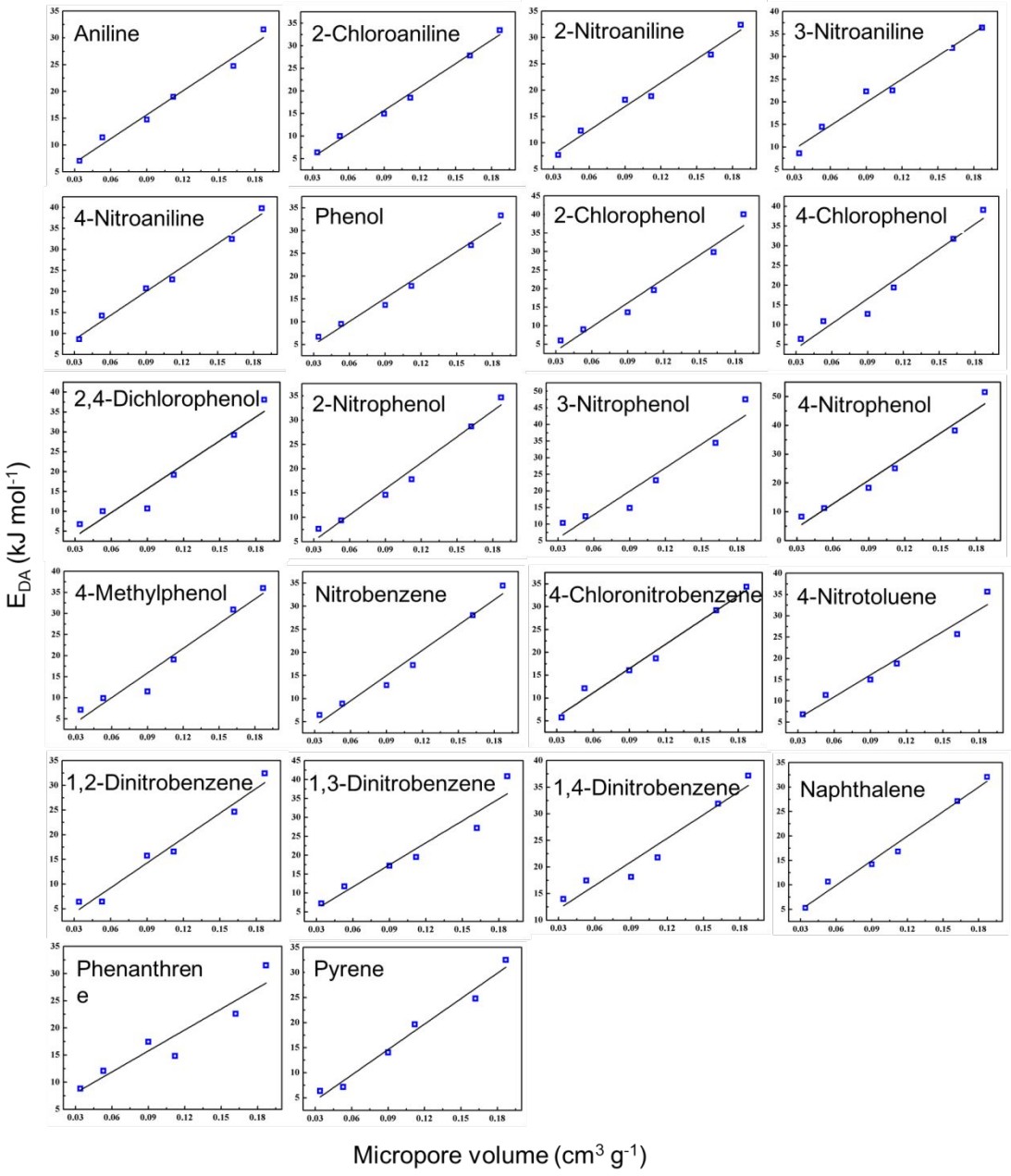

Figure S15. Correlations between micropore volume and E_{DA} values. Solid lines are linear fits.

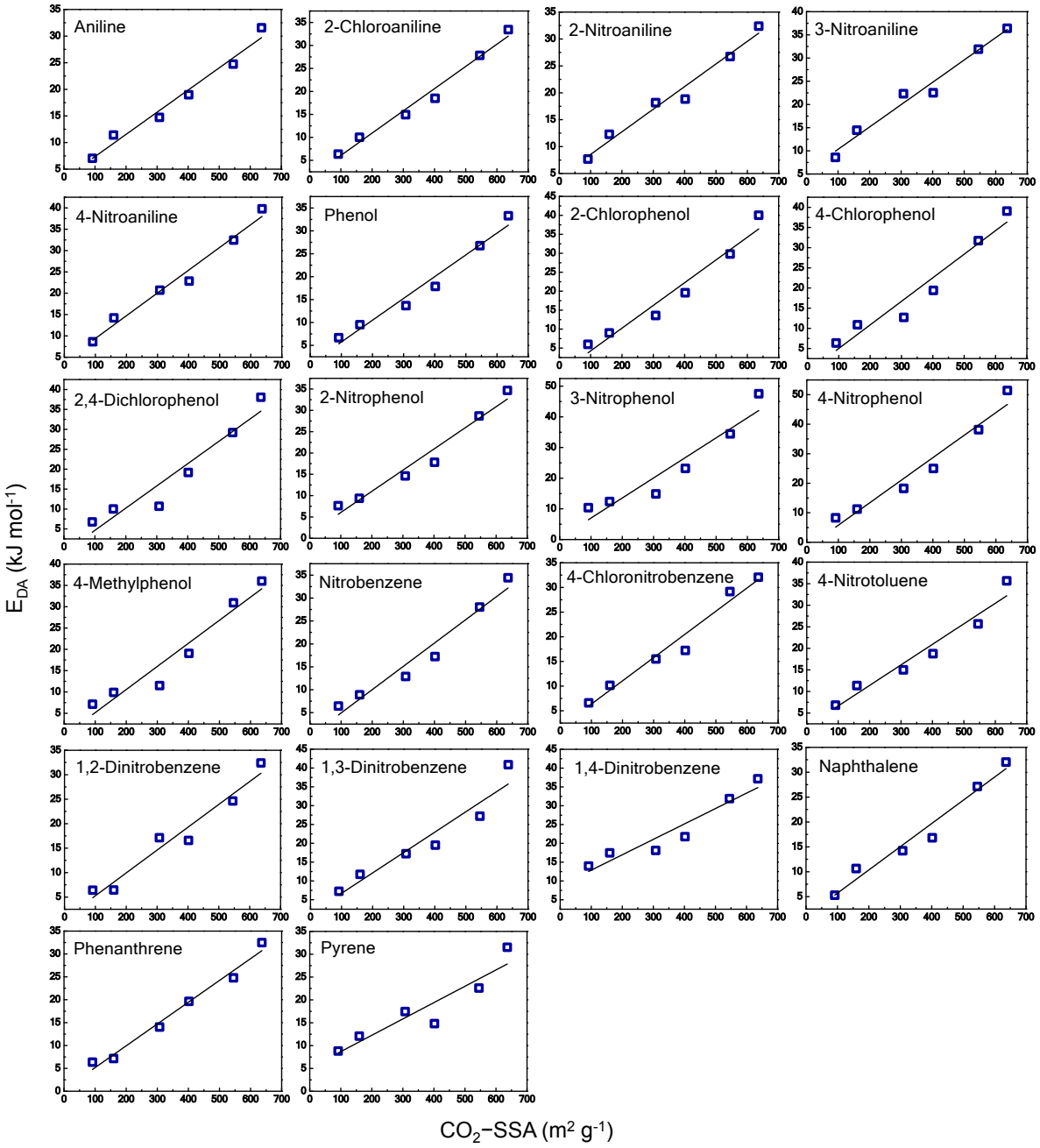

Figure S16. Correlations between CO_2 -SSA and $\boldsymbol{E_{DA}}$ values. Solid lines are linear fits.

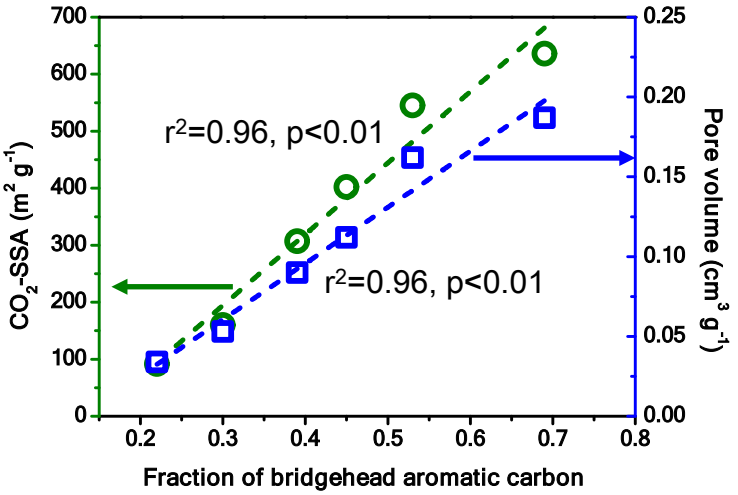

Figure S17. Correlations between fraction of bridgehead aromatic carbon and surface area and micropore volume. Short dot lines are linear fits.

Reference

1. Lattao, C.; Cao, X.; Mao, J.; Schmidt-Rohr, K.; Pignatello, J. J., Influence of Molecular Structure and Adsorbent Properties on Sorption of Organic Compounds to a Temperature Series of Wood Chars. *Environmental Science & Technology* **2014,** *48*, (9), 4790-4798.

2. Cao, X.; Pignatello, J. J.; Li, Y.; Lattao, C.; Chappell, M. A.; Chen, N.; Miller, L. F.; Mao, J., Characterization of Wood Chars Produced at Different Temperatures Using Advanced Solid-State C-13 NMR Spectroscopic Techniques. *Energy & Fuels* **2012,** *26*, (9), 5983-5991.

3. Yang, K.; Yang, J.; Jiang, Y.; Wu, W.; Lin, D., Correlations and adsorption mechanisms of aromatic compounds on a high heat temperature treated bamboo biochar. *Environmental Pollution* **2016,** *210*, 57-64.

4. Willam E, A. J., Thermodynamic properties of organic compounds； enthalpy of fusion and melting point temperature compilation. *Thermochimica Acta* **1991,** *189*, 37-56.

5. Braida, W. J.; Pignatello, J. J.; Lu, Y. F.; Ravikovitch, P. I.; Neimark, A. V.; Xing, B. S., Sorption hysteresis of benzene in charcoal particles. *Environmental Science & Technology* **2003,** *37*, (2), 409-417.

6. Xiao, F.; Pignatello, J. J., Effects of Post-Pyrolysis Air Oxidation of Biomass Chars on Adsorption of Neutral and Ionizable Compounds. *Environmental Science & Technology* **2016,** *50*, (12), 6276-6283.

7. Shen, X.; Guo, X.; Zhang, M.; Tao, S.; Wang, X., Sorption Mechanisms of Organic Compounds by Carbonaceous Materials: Site Energy Distribution Consideration. *Environmental Science & Technology* **2015,** *49*, (8), 4894-4902.

8. Jin, J.; Sun, K.; Wang, Z.; Yang, Y.; Han, L.; Xing, B., Characterization and Phenanthrene Sorption of Natural and Pyrogenic Organic Matter Fractions. *Environmental Science & Technology* **2017,** *51*, (5), 2635-2642.